A MATHEMATICAL SIMULATION OF THE PYROLYSIS OF A MODEL ASPHALTENE

PHILLIP E. SAVAGE[1] AND MICHAEL T. KLEIN

DEPARTMENT OF CHEMICAL ENGINEERING
AND
CENTER FOR CATALYTIC SCIENCE AND TECHNOLOGY
UNIVERSITY OF DELAWARE
NEWARK, DE 19716

[1] PRESENT ADDRESS: UNIVERSITY OF MICHIGAN
DEPARTMENT OF CHEMICAL ENGINEERING
ANN ARBOR, MI 48109

INTRODUCTION

Reaction engineering experiments with coal or heavy oil fractions typically allow observation of only global kinetics and the yields of lumped product fractions; the controlling reaction fundamentals are obscured by the complexity of the reactant and its product spectra. This limitation has motivated experiments with model compounds to help resolve the fundamental reaction pathways, kinetics, and mechanisms involved. These fundamentals are of the model compound reactions, however, and their relation to the reactions of the moieties they mimic in a complex reactant can be vague. Model compound results are often used in the analysis of the reactions of coal or asphaltenes in a qualitative fashion. The object of this paper is to report on a mathematical model of asphaltene pyrolysis which serves as a quantitative bridge between model compounds and actual asphaltenes by combining model-compound deduced reaction pathways and kinetics with aspects of asphaltene structure.

BACKGROUND

Asphaltenes are operationally defined as a response to a solvent extraction protocol. However, the functional groups and chemical moieties they comprise have been probed by numerous spectroscopic and pyrolytic investigations (1-5), and structural scenarios typically include condensed aromatic and heteroaromatic cores to which are attached peripheral alkyl, naphthenic, and heteroatomic substituents. Several of these substituted aromatic cores, referred to as unit sheets, can be bonded together in macromolecular fashion to form an asphaltene particle.

Of the covalent bonds in asphaltene, those in heteroatomic peripheral substituents are the most thermally labile; they are also present in relatively low proportions. C-C bonds in aromatic rings, on the other hand, constitute a large fraction of asphaltene bonds, but they are stable even at very high temperatures. Aliphatic C-C bonds in alkylaromatic, alkylhydroaromatic, and alkylnaphthenic positions are both abundant and reactive and thus constitute the most prevalent thermally scissile groups in asphaltene. Therefore, the reactions (6-10) of the model compounds n-pentadecylbenzene, n-dodecylbenzene, n-butylbenzene, 2-ethylnaphthalene, n-tridecylcyclohexane, and 2-ethyltetralin, mimics of these scissile moieties, seemed a relevant probe of the thermal reactions of the basic hydrocarbon framework of asphaltenes. These model compound data were combined with asphaltene structural information to simulate the pyrolysis of a generic, hypothetical, fully hydrocarbon asphaltene. Structural data used in the model were selected from an overall understanding of asphaltene composition and constitution (8) and were not obtained from spectroscopic characterization of any particular asphaltene. Note however, that the model can readily incorporate structural data from any asphaltene of interest and simulate its pyrolysis specifically.

MODEL DEVELOPMENT

Reactant Asphaltene.

The simulated asphaltene is illustrated schematically in Figure 1. Asphaltenes were regarded (8) as a blend of hydrocarbon particles, defined as covalently bonded oligomers of unit sheets with a degree of polymerization ranging from 1 to 5. The unit sheets comprised between 2 and 30 six-membered rings which could, in turn, be either aromatic or saturated. The maximum number of aromatic rings in a unit sheet was 15, and the number of

saturated rings never exceeded the number of aromatic rings. Peripheral aromatic and saturated carbon atoms in a unit sheet were, respectively, 45% and 25% substituted by aliphatic chains containing from 1 to 25 carbon atoms. A fraction of these chains served as the covalent links which bonded unit sheets into particles, and the balance were terminal substituents.

Four probability distributions describing, respectively, the alkyl substituent chain lengths, the number of aromatic and the number of saturated rings in a unit sheet, and the degree of polymerization of asphaltene particles are displayed in Figure 2. These data were selected such that the average structural parameters for the reactant asphaltene were consistent with values reported in the literature.

In the simulations, the reactant asphaltene consisted of a collection of particles containing the model's basis of 10,000 unit sheets, assembled in a stochastic process. The first step of this assembly was to determine the number of unit sheets in each particle by comparing a random number between 0 and 1 with the integrated probability distribution describing the particle's degree of polymerization (i.e. Fig 2d). The numbers of aromatic and saturated rings in each of the unit sheets in the particle were then determined by comparing independent random numbers with the integrated probability distributions in Figures 2b and 2c. Each saturated ring in the unit sheet was then individually categorized as either hydroaromatic or naphthenic based on whether it was fused to an aromatic ring or exclusively to other saturated rings, respectively. This was accomplished by comparing a random number with the probability, P_H, of a saturated ring being fused to an aromatic ring. P_H was estimated from Equation 1 on the basis that the type of ring (saturated or aromatic) to which a saturated ring was fused was directly proportional to the number of aromatic, N_{ar}, or saturated, N_{nr}, rings in the unit sheet.

$$P_H = \frac{N_{ar}}{N_{ar} + N_{nr} - 1} \tag{1}$$

The numbers of internal and peripheral aromatic and saturated carbon atoms in the unit sheet, defined respectively as those bonded to 3 and to 2 other cyclic carbon atoms, were calculated according to the method of Hirsch and Altgelt (11,12). The number of peripheral atoms of each type was then multiplied by their appropriate degrees of substitution (0.45 and 0.25 for aromatic and saturated carbons, respectively) to calculate the number of peripheral positions containing substituents. The number of peripheral aromatic carbon atoms bearing alkyl chains was then calculated as the total number of substituted aromatic carbon atoms minus the number of peripheral aromatic carbon atoms in hydroaromatic rings. Assembly of the unit sheets was finally completed by comparing a random number with the integrated probability distribution in Figure 2a to determine the number of carbon atoms in each aliphatic substituent. The steps outlined above were repeated for each unit sheet until an entire particle had been constructed. Additional particles were then assembled until 10,000 unit sheets had been included.

Pyrolysis Simulation.

The model compound pyrolyses (8) revealed that ring-opening reactions were of minor consequence for even the saturated rings. Therefore, the polycyclic portion of the unit sheet was modeled as being thermally stable and, hence, conserved during pyrolysis. The only effect of pyrolysis was then to break C-C bonds in the peripheral alkyl substituents and the inter-unit sheet links.

Asphaltene pyrolysis therefore amounted to accounting for the temporal variation of the distribution functions of Figure 2. This was accomplished by 1.) developing differential rate equations for the three reactive moieties (i.e. alkylaromatic, alkylnaphthenic, and alkylhydroaromatic), 2.) integrating these equations numerically with model-compound-deduced rate constants as parameters, 3.) updating the integrated probability distributions to reflect the effects of pyrolysis, and 4.) using the updated distributions to stochastically assemble 10,000 unit sheets which represented the reaction products.

The rate of reaction of an alkylaromatic chain, A_i, of length i in a constant-volume batch reactor was given as Equation 2 where k_{A_i} is the first-order rate constant.

$$\frac{dA_i}{dt} = -k_{A_i} A_i + \sum_{j=1}^{25-i} \nu_{A_{i+j,i}} k_{A_{i+j}} A_{i+j} \tag{2}$$

The two terms on the right hand side account for, respectively, the cleavage of alkylaromatic substituents with i carbon atoms, and the formation of alkylaromatics with i carbons from alkylaromatics containing i+j carbon

atoms where $\nu_{A_{i+j,j}}$ is the stoichiometric coefficient. Completely analogous equations described the rate of reaction of the alkylnaphthenic, N_i, and alkylhydroaromatic, H_i, moieties.

The rate of formation of aliphatic products, AP_i, with i carbon atoms is given by Equation 3, where k and ν are rate constants and stoichiometric coefficients, respectively. Note that secondary reactions of the primary aliphatic products were neglected.

$$\frac{dAP_i}{dt} = \sum_{j=1}^{25-i} (\nu_{A_{i+j,j}} k_{A_{i+j}} A_{i+j} + \nu_{H_{i+j,j}} k_{H_{i+j}} H_{i+j} + \nu_{N_{i+j,j}} k_{N_{i+j}} N_{i+j}) \tag{3}$$

Finally, cleavage of the inter-unit sheet links in the oligomeric particles was described by Equation 4. In modeling the depolymerisation kinetics, all inter-unit sheet linkages were treated as alkylaromatic chains. That is, the rate constant for breaking an inter-unit link was the same as that for cleaving an alkylaromatic substituent.

$$\frac{dP_i}{dt} = -k_{A_i} P_i (i-1) + \sum_{j=1}^{5-i} 2k_{A_{i+j}} P_{i+j} \tag{4}$$

The two terms on the right hand side account for the depolymerization of particles containing i unit sheets, P_i, and the formation of such particles from those with more than i unit sheets, P_{i+j}, respectively.

The rate constants and stoichiometric coefficients required for numerical solution of Equations 2-4 were obtained from the model compound pyrolyses (6-9). For example, the initial product selectivities in pentadecylbenzene (PDB) pyrolysis (6,9) showed that bond scission occurred at the β position about 35% of the time, at the γ position 15% of the time, and at each of the other 12 bonds roughly 4% of the time. These relative proportions for cleavage of each aliphatic bond were modelled to apply to all other alkylaromatics. Similarly, the initial selectivities observed for tridecylcyclohexane (TDC) and 2-ethyltetralin (2ET) pyrolyses (8) provided the stoichiometric coefficients for the alkylnaphthenic and alkylhydroaromatic moieties, respectively.

A unique rate constant for each of the 3 reactive moieties containing from 1 to 25 aliphatic carbons was calculated from the rate constant for the relevant model compound scaled by the square root of the carbon number, as suggested by the apparent first-order rate constant for a Rice-Herzfeld (13) chain. For example, all 15 carbon atom alkylaromatic chains were assumed to follow the pyrolysis kinetics of PDB, and rate constants for alkylaromatic chains with i carbon atoms were calculated as

$$k_{A_i} = k_{PDB} (\frac{i}{15})^{1/2} \tag{5}$$

Although only approximate, Equation 5 correlated available experimental data quite well (8).

To summarise, this mathematical model simulated asphaltene pyrolysis by simultaneously solving 105 differential rate equations; 25 each for cleavage of alkylaromatic, alkylnaphthenic, and alkylhydroaromatic moieties, 25 for the formation of aliphatic products, and 5 for depolymerisation of asphaltene particles. The kinetic parameters in these equations were deduced through model compound pyrolyses. The structural data in the probability distributions, shown in Figure 2 for the reactant asphaltene, were then updated to reflect the effects of pyrolysis, and 10,000 unit sheets were assembled as reaction products.

Reaction Products.

The simulated pyrolyses produced aliphatics, via scission of peripheral moieties on the asphaltenic unit sheet, and product particles containing at least one unit sheet. The product particles were stochastically assembled using the procedure described previously for the reactant asphaltene particles, and they differed from their precursors only in their degree of polymerization and in the length and number of their terminal aliphatic constituents. The polycyclic portion of the unit sheet was thermally stable and hence unaltered by pyrolysis.

To allow comparison with experimentally observed (9,10) temporal variations of solubility-based product fractions from asphaltene pyrolysis, each reaction product from the simulated pyrolyses was assigned to either a gas, maltene, asphaltene, or coke product fraction. Aliphatic products were assigned to the gas fraction if they contained 4 or fewer carbon atoms and to the maltene fraction if they contained more than 4 carbon atoms. The product particles were assigned to one of the solubility-based product fractions on the basis of combinations

of molecular weight and H/C atomic ratio as shown in Table 1. These two parameters provided a physically significant yet convenient means of correlating particle solubility with chemical composition and structure in this model.

MODEL RESULTS

The simulations were of the constant-volume, isothermal, batch pyrolyses of a generic asphaltene and not the particular off-shore California asphaltene used in the experiments. Quantitative agreement between the model and experimental results should not be expected in all cases and treated as a coincidence when found. Note that detailed spectroscopic analysis of any one asphaltene could permit prediction of its reactions, however. Model predictions are presented in terms of the temporal variation of average structural parameters and solubility-based product fractions.

Structural Parameters.

The model monitored the number of each type of aliphatic, aromatic, and naphthenic carbon and hydrogen atoms in the 10,000 unit sheets so that average structural parameters could be determined for the collection of asphaltene particles. The values of selected structural parameters for the reactant asphaltene are reported in Table 2 and are clearly consistent with the ranges of these parameters typically reported in the literature (2,3,14-19) for petroleum asphaltenes.

Figure 3 presents the temporal variation of the particle and unit sheet number average molecular weights, whereas Figure 4 displays the particle molecular weight distribution parameteric in time for simulated asphaltene pyrolysis at 425°C. The particle molecular weight decreased very rapidly and approached the unit sheet average molecular weight, suggesting essentially complete asphaltene depolymerization. Figure 4 shows that the molecular weight distribution for the reactant asphaltene was broad and possessed a high average value and that a significant reduction in average molecular weight and a narrowing of the distribution occurred for asphaltene pyrolysis even at short reaction times.

Experimental data are lacking for a direct quantitative comparison of the model results in Figures 3 and 4, but previous experiments (8) do allow limited scrutiny as follows. Asphaltene pyrolyses at 400°C for 30 min significantly reduced the average molecular weight of the sulfur- and vanadium-containing compounds in asphaltene and shifted the molecular weight distribution to lower values. These results, if generally true for all of the asphaltenic constituents, are in qualitative accord with the model's predictions.

The temporal variation of the H/C atomic ratio and the fraction of carbon atoms being aromatic, f_a, from simulated asphaltene pyrolyses at 425°C are portrayed on Figure 5. The H/C atomic ratio decreased from 1.20 initially to 0.85 at 120 min. The value of f_a, on the other hand, increased from an initial value of 0.42 to 0.61 at 120 min. The predicted variation of the H/C ratio is in good accord with the experimental results from asphaltene pyrolysis at 400°C shown in Figure 6. No experimental data were available for comparison with the temporal variation of f_a.

Product Fractions.

Figure 7 presents the temporal variations of the yields of the gas, maltene, asphaltene, and coke product fractions from simulated asphaltene pyrolyses at 400, 425, and 450°C. Experimental data are provided in Figure 8 for comparison. The simulations at 400°C predicted the experimentally observed induction period for coke production, and maltene and gas yields of the correct order. No experiments were performed at 425°C, but the results of simulated pyrolyses at this temperature closely resembled the experimental results at 400°C. This corroborates the qualitative trends predicted by the model, and further suggests that the model of a generic asphaltene underpredicted the reactivity of the off-shore California asphaltene used in the experiments. The agreement between the model predictions and the experimental temporal variations of the product fractions at 450°C was almost quantitative. Essentially complete asphaltene conversion at 30 minutes, an ultimate coke yield of about 60% that decreased with time, and an ultimate yield of maltenes and gases of about 40% are all common features.

DISCUSSION

The model predictions were consistent with the available experimental data on a qualitative basis without exception, and on a quantitative basis in several instances. This agreement between model and experimental

results is striking because the model deals with a simplified asphaltene structure, includes only model-compound-deduced reaction pathways and kinetics, and contains no kinetics parameters regressed from experiments with actual asphaltenes. The overall consistency of the experimental and simulated asphaltene pyrolyses suggest that the model included many key features of asphaltene structure and its thermal reactivity, and that the pyrolysis kinetics of the model compounds mimicked those of the related moieties in asphaltene.

The model results showed that dealkylation of the asphaltene unit sheets caused the particles to become increasingly hydrogen deficient and more aromatic thereby suggesting an attendant change in their toluene-solubility. Thus as reactant asphaltenes, toluene soluble because of their aliphaticity, were cleaved of their peripheral substituents their toluene solubility diminished, and they eventually appeared as coke in the pyrolysis simulation. The modeling results thus demonstrate that severe overreaction of primary products is not necessary to predict high yields of coke. This corroborates our previous interpretation (10) of the coke fraction as, mainly, a primary pyrolysis product containing the polycyclic cores of asphaltenic unit sheets.

Finally, the model results also permit speculation into the role of pyrolysis in nominally catalytic asphaltene hydroprocessing reactions. The simulations showed that asphaltene depolymerization occurred even at short reaction times and that many particles existed as single unit sheets rather than covalently bonded oligomers thereof. These individual asphaltene unit sheets, which are much smaller than the macromolecular particles, will be major participants in catalytic reactions because they can more readily diffuse within the porous catalyst. This suggests that catalytic hydroprocessing at high temperatures will be of thermally derived asphaltene fragments and not the asphaltene particle itself.

LITERATURE CITED

1 Yen, T. F. in Chemistry of Asphaltenes, ACS Adv. Chem. Ser. No. 195 **1981**, 39.

2 Yen, T. F., Wu, W. H., Chilingar, G. V. *Energy Sources* **1984**, 7, 203.

3 Yen, T. F., Wu, W. H., Chilingar, G. V. *Energy Sources* **1984**, 7, 275.

4 Speight, J. G., Moschopedis, S. E. in Chemistry of Asphaltenes, ACS Adv. Chem. Ser. No. 195 **1981**, 1.

5 Koots, J. A., Speight, J. G. *Fuel* **1975**, 54, 179.

6 Savage, P. E., Klein, M. T. *Ind. Eng. Chem. Research* **1987**, in press.

7 Savage, P. E., Klein, M. T. *Ind. Eng. Chem. Research* **1987**, 26, 374.

8 Savage, P. E. *Ph.D. Dissertation* University of Delaware **1986**

9 Savage, P. E., Klein, M. T., Kukes, S. G. *ACS Div. Fuel Chem. Prepr.* **1985** 30, 408.

10 Savage, P. E., Klein, M. T., Kukes, S. G. *Ind. Eng. Chem. Process Des. Dev.* **1985**, 24, 1169.

11 Hirsch, E., Altgelt, K. H. *Anal. Chem.* **1970**, 42, 1330.

12 Hirsch, E. *Anal. Chem.* **1970**, 42, 1326.

13 Rice, F. O., Herzfeld, K. F. *J. Am. Chem. Soc.* **1934**, 56, 284.

14 Ali, L. H., Al-Ghannam, K. A. *Fuel* **1981**, 60, 1043.

15 Boduszynski, M. M., Chadha, B. R., Szkuta-Pochopien, T. *Fuel* **1977**, 56, 443.

16 Speight, J. G. *Fuel* **1970**, 49, 134.

17 Speight, J. G. *Fuel* **1971**, 50, 102.

18 Suzuki, T., Itoh, M., Takegami, Y., Watanabe, Y. *Fuel* **1982**, 61, 402.

19 Yen, T. F. *Energy Sources* **1974**, 1, 447.

TABLE ONE

CRITERIA FOR ASSIGNING PARTICLES TO PRODUCT FRACTIONS

Criteria	Product Fraction	Operational Definition
MW < 300 and H/C > 1.0	Maltene	heptane - soluble
MW > 300 and H/C > 1.0	Asphaltene	heptane - insoluble
MW < 300 and H/C < 1.0		toluene - soluble
MW > 300 and H/C < 1.0	Coke	toluene - insoluble

TABLE TWO

AVERAGE STRUCTURAL PARAMETERS FOR PETROLEUM ASPHALTENE

Parameter	Significance	Model	Literature (1-5, 14-19)
H/C	atomic ratio	1.20	1.09 - 1.29
f_a	fraction of C atoms in aromatic rings	0.42	0.30 - 0.61
f_n	fraction of C atoms in saturated rings	0.13	0.06 - 0.24
H_a	fraction of H atoms in aromatic rings	0.09	0.04 - 0.11
H_n	fraction of H atoms in saturated rings	0.16	0.16 - 0.19
C_p/C_a	peripheral aromatic carbons / total aromatic carbons (shape of aromatic core)	0.48	0.31 - 0.55
C_s/C_{sa}	total saturated carbons / saturated carbons α to ring (average alkyl chain length)	4.93	3.1 - 8.4
C_{sa}/C_p	saturated carbons α to ring / peripheral aromatic carbons (degree of substitution of aromatics in unit sheet)	0.45	0.39 - 0.65

Figure 1: Structural Hierarchy in Pyrolysis Model

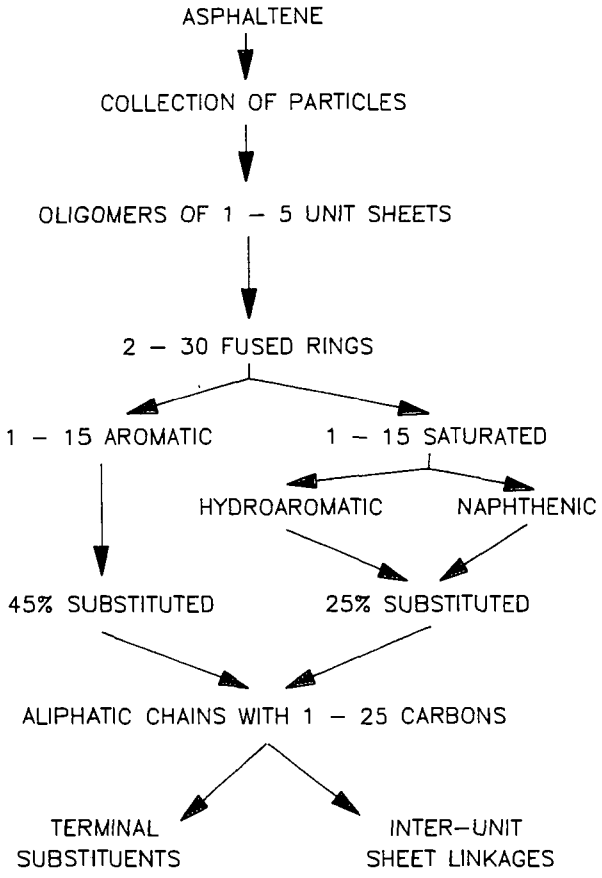

Figure 2: Integrated Distributions for Elements of Asphaltene Structure

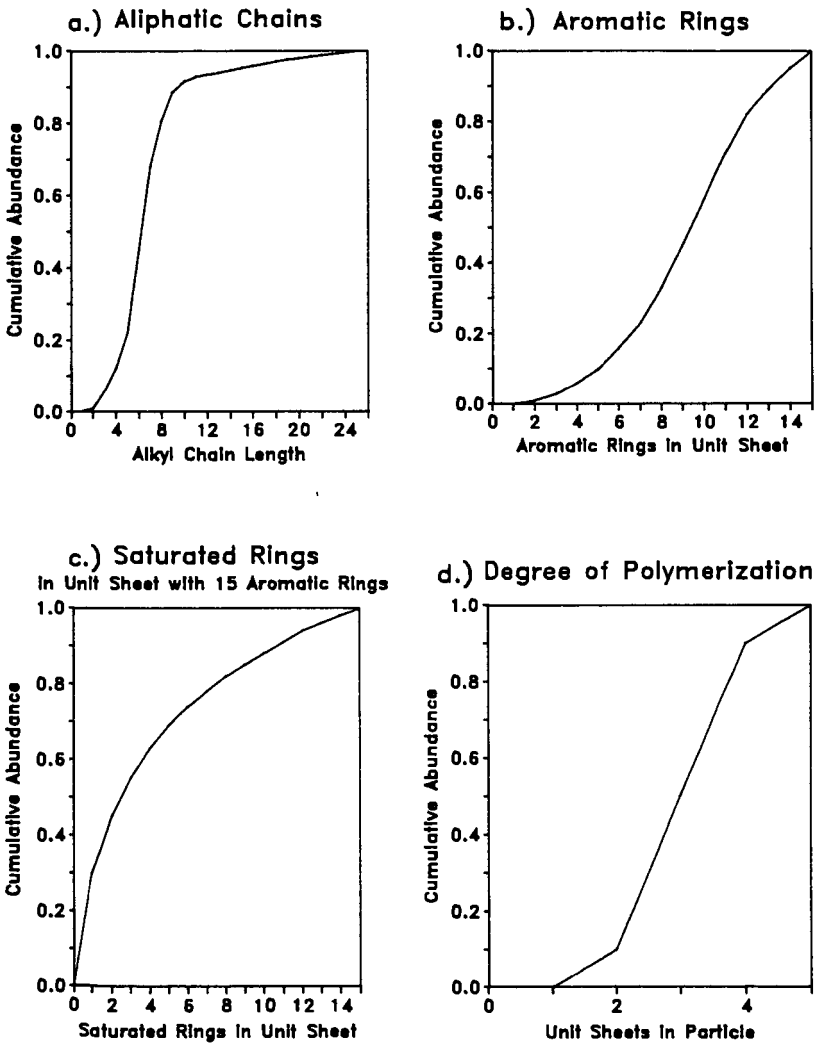

Figure 3: Temporal Variation of MW

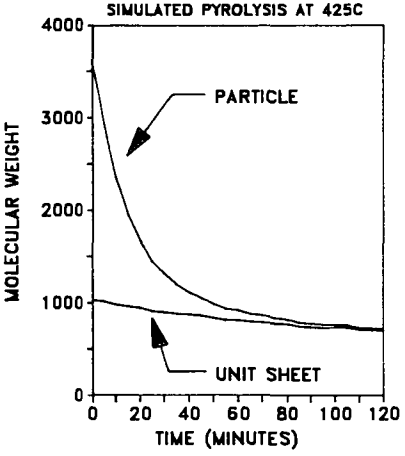

Figure 4: Molecular Weight Distributions

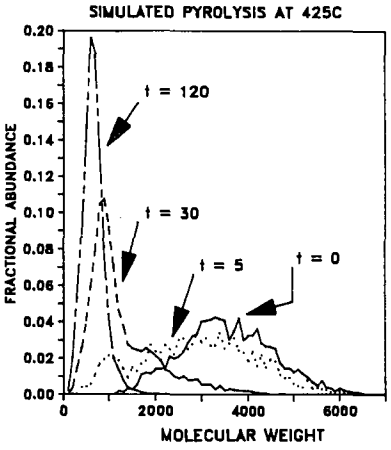

Figure 5: Temporal Variation of H/C and f_a

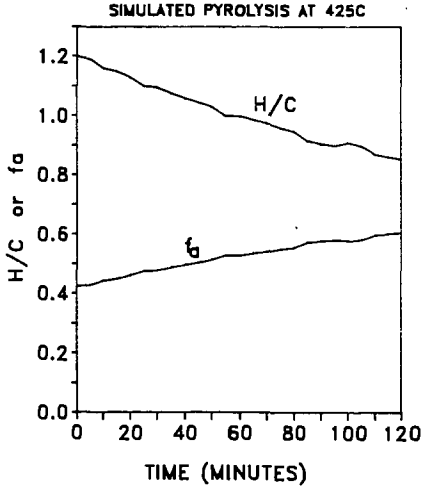

Figure 6: Temporal Variation of H/C

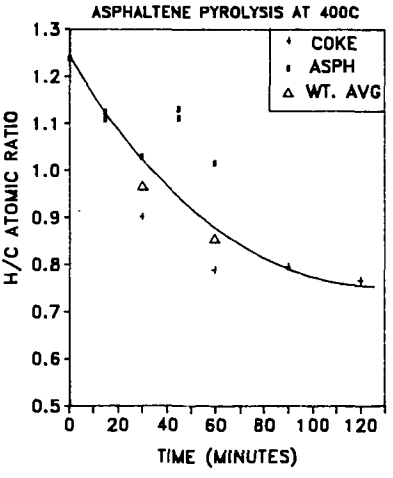

Figure 7: Temporal Variation of Product Fractions
from Simulated Asphaltene Pyrolysis

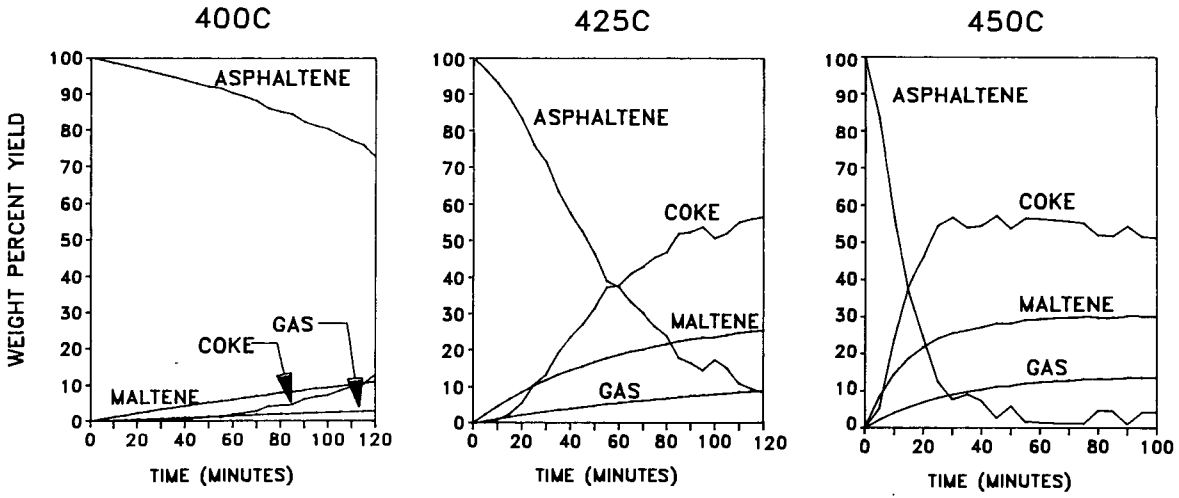

Figure 8: Temporal Variation of Product Fractions from Asphaltene Pyrolysis